

${}^3\text{H}$ production via neutron-neutron-deuteron recombination

A. Deltuva and A. C. Fonseca

Centro de Física Nuclear da Universidade de Lisboa, P-1649-003 Lisboa, Portugal

(Received August 7, 2018)

We study the recombination of two neutrons and deuteron into neutron and ${}^3\text{H}$ using realistic nucleon-nucleon potential models. Exact Alt, Grassberger, and Sandhas equations for the four-nucleon transition operators are solved in the momentum-space framework using the complex-energy method with special integration weights. We find that at astrophysical or laboratory neutron densities the production of ${}^3\text{H}$ via the neutron-neutron-deuteron recombination is much slower as compared to the radiative neutron-deuteron capture. We also calculate neutron- ${}^3\text{H}$ elastic and total cross sections.

PACS numbers: 21.45.-v, 25.10.+s, 21.30.-x

I. INTRODUCTION

The nonrelativistic quantum mechanics solution of the four-nucleon scattering problem has, in the past five years, reached a level of sophistication and numerical accuracy that makes it a natural theoretical laboratory to study nucleon-nucleon (NN) force models with the same confidence as one has used the three-nucleon system in the past. This has been demonstrated in a recent benchmark for n - ${}^3\text{H}$ and p - ${}^3\text{He}$ elastic scattering observables [1], where three different theoretical frameworks have been compared, namely, the hyperspherical harmonics (HH) expansion method [2, 3], the Faddeev-Yakubovsky (FY) equations [4] for the wave function components in coordinate space [5, 6], and the Alt, Grassberger and Sandhas (AGS) equations [7] for transition matrices that were solved in the momentum space [8, 9]. All methods include not only the hadronic NN interaction, but also the Coulomb repulsion between protons. While the first two methods have the advantage of being able to deal with charged-particle reactions at very low energies and include static three-nucleon forces (3NF), the third one is the only method so far to make predictions for multi-channel reactions such as $d+d \rightarrow d+d$, $d+d \rightarrow n+{}^3\text{He}$, $d+d \rightarrow p+{}^3\text{H}$, and $p+{}^3\text{H} \rightarrow n+{}^3\text{He}$ (and the corresponding inverse reactions) [10, 11].

In a previous publication [12] a major step was taken in extending the AGS calculations above three- and four-cluster breakup thresholds. Owing to the complicated analytic structure of the four-body kernel above breakup threshold the calculations were performed using the complex energy method [13, 14] whose accuracy and practical applicability was greatly improved by a special integration method [12]. This allowed us to achieve fully converged results for n - ${}^3\text{H}$ elastic scattering with realistic NN interactions. We note that the FY calculations of n - ${}^3\text{H}$ elastic scattering have been recently extended as well to energies above the four-nucleon breakup threshold [15], however, using a semi-realistic NN potential limited to S -waves.

In the present work we extend the method of Ref. [12] to calculate the neutron-neutron-deuteron (nnd) recombination into $n+{}^3\text{H}$ and its time-reverse reaction, i.e.,

the three-cluster breakup $n+{}^3\text{H} \rightarrow n+n+d$. Although breakup reactions are usually measured in nuclear physics, the recombination has the advantage that its rate is finite at threshold where the breakup cross section vanishes due to phase-space factors. Furthermore, $n+n+d \rightarrow n+{}^3\text{H}$ is the only hadronic recombination reaction in the four-nucleon system that at threshold is not suppressed by the Coulomb barrier (like $n+p+d \rightarrow p+{}^3\text{H}$) or Pauli repulsion (like $n+n+n+p \rightarrow n+{}^3\text{H}$). It can take place in any environment with neutrons and deuterons and, with respect to the tritium synthesis, it may be competitive to the electromagnetic capture reaction $n+d \rightarrow \gamma+{}^3\text{H}$. Thus, one may rise the question at what conditions the $n+n+d \rightarrow n+{}^3\text{H}$ recombination would dominate over the $n+d \rightarrow \gamma+{}^3\text{H}$ radiative capture and to what extent it is relevant for astrophysical processes.

In addition, we also present results for the $n+{}^3\text{H}$ elastic scattering and study the energy dependence of the total $n+{}^3\text{H}$ cross section.

II. 4N SCATTERING EQUATIONS

We use the time-reversal symmetry to relate the nnd recombination amplitude to the three-cluster breakup amplitude of the initial n - ${}^3\text{H}$ state, i.e.,

$$\langle \Phi_1 | T_{13} | \Phi_3 \rangle = \langle \Phi_3 | T_{31} | \Phi_1 \rangle. \quad (1)$$

Here $|\Phi_1\rangle$ is the n - ${}^3\text{H}$ channel state and $|\Phi_3\rangle$ is the nnd channel state. The advantage is that the three-cluster breakup amplitude $\langle \Phi_3 | T_{31} | \Phi_1 \rangle$ is more directly related to the AGS transition operators $\mathcal{U}_{\beta\alpha}$ calculated in our previous works [8, 12]. Since we use the isospin formalism where the nucleons are treated as identical fermions, there are only two distinct two-cluster partitions, namely, $\beta, \alpha = 1$ corresponds to the $3+1$ partition $(12,3)4$ whereas $\beta = 2$ corresponds to the $2+2$ partition $(12)(34)$. For the initial n - ${}^3\text{H}$ state we need only $\mathcal{U}_{\beta 1}$, i.e., we solve the AGS equations for the four-nucleon transition oper-

ators

$$\begin{aligned} \mathcal{U}_{11} = & -(G_0 t G_0)^{-1} P_{34} - P_{34} U_1 G_0 t G_0 \mathcal{U}_{11} \\ & + U_2 G_0 t G_0 \mathcal{U}_{21}, \end{aligned} \quad (2a)$$

$$\mathcal{U}_{21} = (G_0 t G_0)^{-1} (1 - P_{34}) + (1 - P_{34}) U_1 G_0 t G_0 \mathcal{U}_{11}. \quad (2b)$$

The free resolvent with the complex energy parameter $Z = E + i\varepsilon$ and the free Hamiltonian H_0 is

$$G_0 = (Z - H_0)^{-1} \quad (3)$$

whereas the pair (12) transition matrix

$$t = v + v G_0 t \quad (4)$$

is derived from the respective potential v . The 3+1 and 2+2 subsystem transition operators are obtained from the integral equations

$$U_\alpha = P_\alpha G_0^{-1} + P_\alpha t G_0 U_\alpha. \quad (5)$$

The basis states are antisymmetric under exchange of the two nucleons (12). In the 2 + 2 partition the basis states have to be antisymmetric also under exchange of the two nucleons (34). The full antisymmetry as required for the four-nucleon system is ensured by the permutation operators P_{ab} of nucleons a and b with $P_1 = P_{12} P_{23} + P_{13} P_{23}$ and $P_2 = P_{13} P_{24}$.

The n - ^3H elastic and inelastic reaction amplitudes at the available energy $E = \epsilon_1 + p_1^2/2\mu_1$ are obtained in the limit $\varepsilon \rightarrow +0$. Here ϵ_1 is the ^3H ground state energy, \mathbf{p}_1 is the relative n - ^3H momentum, and $\mu_1 = 3m_N/4$, m_N being the nucleon mass. The elastic scattering amplitude is calculated in Refs. [8, 12]. The amplitude for the nnd breakup is obtained by the antisymmetrization of the general three-cluster breakup amplitude [16], resulting

$$\begin{aligned} \langle \Phi_3 | T_{31} | \Phi_1 \rangle = & \sqrt{3} \langle \Phi_3 | [(1 - P_{34}) U_1 G_0 t G_0 \mathcal{U}_{11} \\ & + U_2 G_0 t G_0 \mathcal{U}_{21}] | \phi_1 \rangle. \end{aligned} \quad (6)$$

Here $|\phi_1\rangle$ is the Faddeev component of the n - ^3H channel state $|\Phi_1\rangle = (1 + P_1)|\phi_1\rangle$; ϵ_1 and $|\phi_1\rangle$ are obtained by solving the bound-state Faddeev equation

$$|\phi_1\rangle = G_0 t P_1 |\phi_1\rangle \quad (7)$$

at $\varepsilon \rightarrow +0$.

We solve the AGS equations (2) in the momentum-space partial-wave framework. The momentum and angular momentum part of the basis states are $|k_x k_y k_z [l_z \{ \{ l_x S_x \} j_x s_y \} S_y \} J_y s_z] S_z \mathcal{J} \mathcal{M}\rangle$ for the 3 + 1 configuration and $|k_x k_y k_z (l_z \{ \{ l_x S_x \} j_x [l_y (s_y s_z) S_y] j_y \} S_z) \mathcal{J} \mathcal{M}\rangle$ for the 2 + 2. Here k_x , k_y , and k_z are the four-particle Jacobi momenta as given in Ref. [17], l_x , l_y , and l_z are the corresponding orbital angular momenta, j_x and j_y are the total angular momenta of pairs (12) and (34), J_y is

the total angular momentum of the (123) subsystem, s_y and s_z are the spins of nucleons 3 and 4, S_x , S_y , and S_z are the channel spins of two-, three-, and four-particle systems, and \mathcal{J} is the total angular momentum with the projection \mathcal{M} . We include a large number of four-nucleon partial waves, $l_x, l_y, l_z, j_x, j_y, J_y \leq 4$ and $\mathcal{J} \leq 5$, such that the results are well converged. The complex-energy method [13] with special integration weights [12] is used to treat the singularities of the AGS equations (2). To obtain accurate results for the breakup amplitude $\langle \Phi_3 | T_{31} | \Phi_1 \rangle$ near the nnd threshold we had to use $0.1 \text{ MeV} \leq \varepsilon \leq 0.4 \text{ MeV}$ that are smaller than $1.0 \text{ MeV} \leq \varepsilon \leq 2.0 \text{ MeV}$ used in the elastic scattering calculations of Ref. [12]. However, the need for relatively small ε values caused no technical problems since the integration with special weights [12] provides very accurate treatment of the ^3H pole whereas the quasi-singularities due to deuteron pole are located in a very narrow region with very small weight, such that about 30 grid points for the discretization of each momentum variable were sufficient.

III. RESULTS

The nnd recombination rate K_3 is defined such that the number of recombination events per volume and time is $K_3 \rho_n^2 \rho_d$ with ρ_n (ρ_d) being the density of neutrons (deuterons). We calculate it as a function of the relative nnd kinetic energy $E_3 = E - \epsilon_d$, i.e.,

$$\begin{aligned} K_3 = & \frac{(2\pi)^7 \mu_1 p_1}{g_3 \pi^2 (\mu_{\alpha y} \mu_\alpha)^{3/2} E_3^2} \sum_{m_s} \int d^3 k_y d^3 k_z \\ & \times |\langle \Phi_3 | T_{31} | \Phi_1 \rangle|^2 \delta \left(E_3 - \frac{k_y^2}{2\mu_{\alpha y}} - \frac{k_z^2}{2\mu_\alpha} \right). \end{aligned} \quad (8)$$

Here $\epsilon_d = -2.2246 \text{ MeV}$ is the deuteron bound state energy, $\mu_{\alpha y}$ and μ_α are the reduced masses associated with the four-nucleon Jacobi momenta k_y and k_z . For example, in the 2+2 configuration k_y is the relative momentum of the two neutrons while k_z is the relative momentum between the center of mass (c.m.) of the two-neutron subsystem and the deuteron. The nnd state can be represented in both 3+1 and 2+2 configurations equally well; $\mu_{\alpha y} \mu_\alpha = m_N^2/2$. The sum in Eq. (8) runs over all initial and final spin projections m_s that are not explicitly indicated in our notation for the channel states while $g_3 = 12$ takes care of the spin averaging in the initial nnd state. The integral in Eq. (8), up to a factor, determines also the total cross section σ_3 for the three-cluster breakup of the initial n - ^3H state. Thus, the nnd recombination rate can be related to σ_3 as

$$K_3 = \frac{8\pi g_1 p_1^2}{g_3 (\mu_{\alpha y} \mu_\alpha)^{3/2} E_3^2} \sigma_3 \quad (9)$$

where $g_1 = 4$ is the number of n - ^3H spin states. Below the four-nucleon breakup threshold σ_3 can be obtained

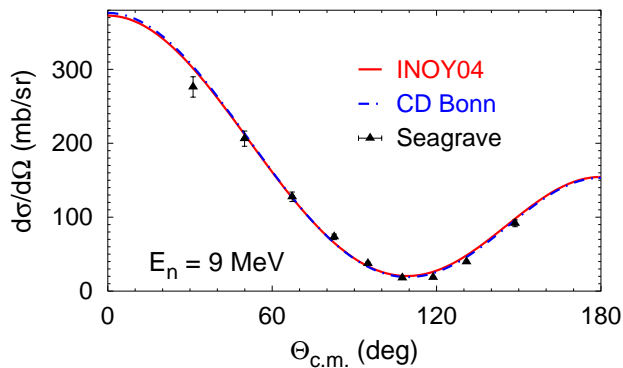


FIG. 1. (Color online) Differential cross section for elastic n - ${}^3\text{H}$ scattering at 9 MeV neutron energy as a function of c.m. scattering angle. Results obtained with INOY04 (solid curves) and CD Bonn (dashed-dotted curves) potentials are compared with the experimental data from Ref. [22].

via the optical theorem as a difference between the total and elastic cross sections. The equation (9) cannot be used right at the nnd threshold where both E_3 and σ_3 vanish. For $E_3 \rightarrow 0$ the nnd recombination rate (8) becomes

$$K_3^0 = \frac{4\pi}{g_3} (2\pi)^7 \mu_1 p_1 \sum_{m_s} |\langle \Phi_3^0 | T_{31} | \Phi_1 \rangle|^2, \quad (10)$$

where for the channel state $|\Phi_3^0\rangle$ the relative momenta $k_y = k_z = 0$. The most convenient representation for $|\Phi_3^0\rangle$ is a single-component $2+2$ state with $l_y = l_z = S_y = j_y = 0$ and $j_x = S_z = \mathcal{J} = 1$.

We study the four-nucleon system using realistic high-precision two-nucleon potentials, namely, the inside-nonlocal outside-Yukawa (INOY04) potential by Doleschall [5, 18], the Argonne (AV18) potential [19], the charge-dependent Bonn potential (CD Bonn) [20], and its extension CD Bonn + Δ [21] allowing for an excitation of a nucleon to a Δ isobar and thereby yielding effective three- and four-nucleon forces. Among these potentials only INOY04 nearly reproduces experimental binding energy of ${}^3\text{H}$ (8.48 MeV), while AV18, CD Bonn and CD Bonn + Δ underbind the ${}^3\text{H}$ nucleus by 0.86, 0.48 and 0.20 MeV, respectively.

First we study the n - ${}^3\text{H}$ reactions for existing experimental data. We concentrate on the energy regime relevant for the nnd recombination, i.e., between the three- and four-cluster breakup thresholds. In Fig. 1 we show the differential cross section for n - ${}^3\text{H}$ elastic scattering at $E_n = 9$ MeV neutron energy corresponding to $E_3 = 0.49$ MeV. The predictions agree well with the experimental data of Ref. [22] and are quite insensitive to the choice of the potential. Results for n - ${}^3\text{H}$ elastic scattering above the four-cluster breakup threshold up to $E_n = 22.1$ MeV are given in Ref. [12].

In Fig. 2 we show the total cross section for n - ${}^3\text{H}$ scattering at neutron energies ranging from 0 to 22 MeV

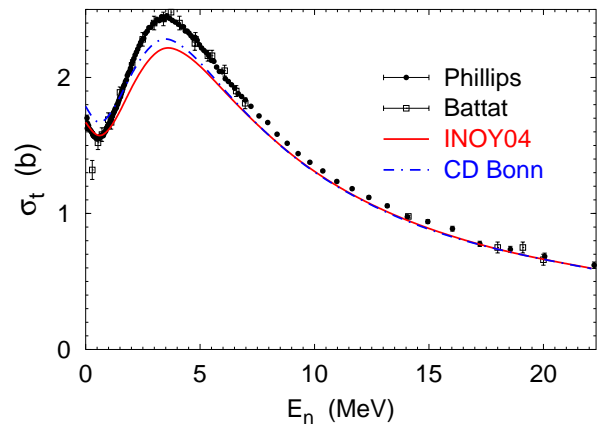


FIG. 2. (Color online) Total cross section for n - ${}^3\text{H}$ scattering as a function of the neutron lab energy. Results obtained with INOY04 (solid curves) and CD Bonn (dashed-dotted curves) potentials are compared with the experimental data from Refs. [23, 24].

and compare it to the data of Refs. [23, 24]. The three-cluster (four-cluster) breakup threshold corresponds to $E_n = 8.35$ (11.31) MeV. As already found in Refs. [5, 8, 25], the total n - ${}^3\text{H}$ cross section around the low-energy peak is underpredicted by the traditional two-nucleon potentials while the low-momentum or chiral effective field theory potentials may provide a better description [26, 27]. Although with increasing energy the predictions approach the experimental data, as already mentioned [8], the elastic and total cross section data may be inconsistent. In the low-energy regime where the inelastic cross section should vanish for $E_n \leq 8.35$ MeV and remain very small at $E_n = 9$ MeV, there is in general a better agreement between predictions and experiment for the elastic differential cross section than for the total cross section which is significantly underestimated by theory. A solution to this discrepancy may require new measurements in this energy regime.

In Fig. 3 we study the energy-dependence of the nnd recombination rate in the standard form $N_A^2 K_3$ where N_A is the Avogadro's number. We show only INOY04 predictions as it is the only used potential with correct ϵ_1 and p_1 values. The results at $E_3 = 0$ are obtained from Eq. (10) while at $E_3 > 0$ it was more convenient to use Eq. (9) where σ_3 was calculated using optical theorem. Thus, for $E_3 > |\epsilon_d|$ our predictions in Fig. 3 estimate the upper limit for $N_A^2 K_3$ since they assume that the four-cluster breakup cross section is much smaller than the three-cluster breakup cross section. In the relevant energy regime $0 \leq E_3 \leq |\epsilon_d|$ the nnd recombination rate increases with increasing energy E_3 nearly linearly due to the increasing contributions of partial waves with nonzero orbital angular momentum l_z . The threshold values $N_A^2 K_3^0$ referring to all employed potentials are collected in Table I; they increase with ${}^3\text{H}$ binding energy.

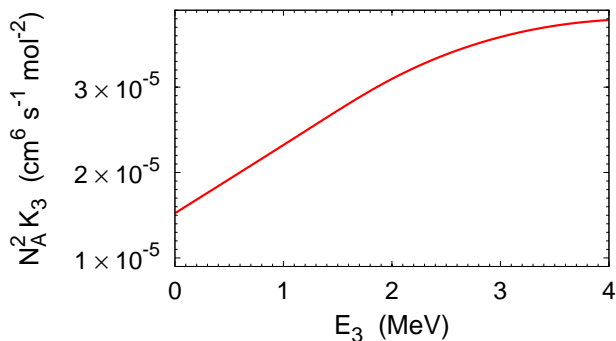


FIG. 3. (Color online) nnd recombination rate K_3 as a function of relative kinetic nnd energy E_3 . Predictions are obtained using the INOY04 potential.

	$ \epsilon_1 $ (MeV)	$N_A^2 K_3^0$ ($\text{cm}^6 \text{s}^{-1} \text{mol}^{-2}$)
AV18	7.62	1.31×10^{-5}
CD Bonn	8.00	1.41×10^{-5}
CD Bonn + Δ	8.28	1.47×10^{-5}
INOY04	8.49	1.52×10^{-5}

TABLE I. nnd recombination rate at threshold calculated with different two-nucleon potentials. The values for ${}^3\text{H}$ binding energy are listed as well.

Finally we compare the relative importance of the nnd recombination and nd radiative capture. For the latter the number of events, i.e., the number of produced ${}^3\text{H}$ nuclei per volume and time is $K_2 \rho_n \rho_d$ with K_2 being the nd capture rate. The threshold value for it given in Ref. [28] is $N_A K_2^0 = 66.2 \text{ cm}^3 \text{ s}^{-1} \text{ mol}^{-1}$. The critical density of neutrons at which both processes yield comparable contributions to the ${}^3\text{H}$ production in the low-energy (low-temperature) limit is given by $\rho_n^c = K_2^0 / K_3^0 \approx 2.6 \times 10^{30} \text{ cm}^{-3}$. This corresponds to the mass density of $4.4 \times 10^6 \text{ g/cm}^3$. Thus, one may conclude that at the neutron density available in the laboratories (such as National Ignition Facility with expected $\rho_n \sim 10^{22}$ to 10^{25} cm^{-3} [29]) the nnd recombi-

nation is entirely irrelevant as well as for the big-bang nucleosynthesis where the estimated baryon density is even lower. On the other hand, the neutron density in core-collapse supernova or neutron stars may be higher than ρ_n^c by several orders of magnitude but the absence of deuterons renders $n + d$ and $n + n + d$ reactions irrelevant. However, based on our results one may conjecture that at such high densities the three-cluster recombination of two neutrons and a heavier nucleus A , i.e., $n + n + A \rightarrow n + (An)$ might be as important as the corresponding radiative capture $n + A \rightarrow \gamma + (An)$. For example, the above reactions with A being ${}^{20}\text{Ne}$ are relevant for the neon-burning process.

IV. SUMMARY

We have solved the four-nucleon AGS equations in the energy regime above the three-cluster threshold and studied the rate for the recombination reaction $n + n + d \rightarrow n + {}^3\text{H}$. The obtained results show that the nnd recombination is not competitive with the radiative nd capture for the production of tritium at neutron densities available in laboratory induced fusion or astrophysical processes. Thus, one may conjecture with a confidence that other nucleon-nucleon-deuteron recombination reactions (for example, $p + p + d \rightarrow p + {}^3\text{He}$ that could contribute to the hydrogen burning process in stars), being in addition suppressed by the Coulomb repulsion, are inferior to the respective nucleon-deuteron radiative capture reactions at realistic densities, and that four-nucleon recombination reactions are even far less relevant.

In addition, we presented results for the n - ${}^3\text{H}$ elastic differential cross section at $E_n = 9 \text{ MeV}$ and the n - ${}^3\text{H}$ total cross section up to $E_n = 22 \text{ MeV}$. While the elastic cross section agrees fairly well with the data, there is a disagreement for the total cross section, especially in the low-energy regime. This indicates a possible inconsistencies between the n - ${}^3\text{H}$ elastic and total cross section data and calls for new measurements.

ACKNOWLEDGMENTS

The authors thank J. A. Frenje for discussions.

-
- [1] M. Viviani, A. Deltuva, R. Lazauskas, J. Carbonell, A. C. Fonseca, A. Kievsky, L. E. Marcucci, and S. Rosati, Phys. Rev. C **84**, 054010 (2011).
 - [2] M. Viviani, A. Kievsky, S. Rosati, E. A. George, and L. D. Knutson, Phys. Rev. Lett. **86**, 3739 (2001).
 - [3] A. Kievsky, S. Rosati, M. Viviani, L. E. Marcucci, and L. Girlanda, J. Phys. G **35**, 063101 (2008).
 - [4] O. A. Yakubovsky, Yad. Fiz. **5**, 1312 (1967) [Sov. J. Nucl. Phys. **5**, 937 (1967)].
 - [5] R. Lazauskas and J. Carbonell, Phys. Rev. C **70**, 044002 (2004).
 - [6] R. Lazauskas, Phys. Rev. C **79**, 054007 (2009).
 - [7] P. Grassberger and W. Sandhas, Nucl. Phys. **B2**, 181 (1967); E. O. Alt, P. Grassberger, and W. Sandhas, JINR report No. E4-6688 (1972).
 - [8] A. Deltuva and A. C. Fonseca, Phys. Rev. C **75**, 014005 (2007).
 - [9] A. Deltuva and A. C. Fonseca, Phys. Rev. Lett. **98**, 162502 (2007).
 - [10] A. Deltuva and A. C. Fonseca, Phys. Rev. C **76**, 021001(R) (2007).
 - [11] A. Deltuva and A. C. Fonseca, Phys. Rev. C **81**, 054002 (2010).

- (2010).
- [12] A. Deltuva and A. C. Fonseca, Phys. Rev. C **86**, 011001(R) (2012).
- [13] H. Kamada, Y. Koike, and W. Glöckle, Prog. Theor. Phys. **109**, 869L (2003).
- [14] E. Uzu, H. Kamada, and Y. Koike, Phys. Rev. C **68**, 061001(R) (2003).
- [15] R. Lazauskas, Phys. Rev. C **86**, 044002 (2012).
- [16] A. Deltuva, Few-Body Syst. DOI:10.1007/s00601-012-0477-0; arXiv:1207.6921.
- [17] A. Deltuva, Phys. Rev. A **85**, 012708 (2012).
- [18] P. Doleschall, Phys. Rev. C **69**, 054001 (2004).
- [19] R. B. Wiringa, V. G. J. Stoks, and R. Schiavilla, Phys. Rev. C **51**, 38 (1995).
- [20] R. Machleidt, Phys. Rev. C **63**, 024001 (2001).
- [21] A. Deltuva, R. Machleidt, and P. U. Sauer, Phys. Rev. C **68**, 024005 (2003).
- [22] J. Seagrave, J. Hopkins, D. Dixon, P. K. Jr., E. Kerr, A. Niiler, R. Sherman, and R. Walter, Annals of Physics **74**, 250 (1972).
- [23] M. E. Battat *et al.*, Nucl. Phys. **12**, 291 (1959).
- [24] T. W. Phillips, B. L. Berman, and J. D. Seagrave, Phys. Rev. C **22**, 384 (1980).
- [25] R. Lazauskas, J. Carbonell, A. C. Fonseca, M. Viviani, A. Kievsky, and S. Rosati, Phys. Rev. C **71**, 034004 (2005).
- [26] A. Deltuva, A. C. Fonseca, and S. K. Bogner, Phys. Rev. C **77**, 024002 (2008).
- [27] M. Viviani, L. Girlanda, A. Kievsky, L. E. Marcucci, and S. Rosati, EPJ Web of Conferences **3**, 05011 (2010).
- [28] W. A. Fowler, G. R. Caughlan, and B. A. Zimmerman, Annu. Rev. Astron. Astrophys. **5**, 525 (1967).
- [29] J. A. Frenje, private communication.